Downloaded from www.ajronline.org by MIT Libraries on 05/02/24 from IP address 18.116.164.246. Copyright ARRS. For personal use only; all rights reserved

Residents
inRadiology

Upper Lobe–Predominant Diseases of the Lung

Stefan F. Nemec[1]
Alexander A. Bankier
Ronald L. Eisenberg

The lung is a fundamentally heterogeneous organ because of differences in perfusion-ventilation ratio, lymphatic flow, metabolism, and mechanics, all of which result from the influence of gravity. These physiologic disparities have been recognized as important factors determining the upper lobe predominance of certain pulmonary diseases.

In an erect individual, the lung apex is relatively overventilated (ratio of ventilation to perfusion, 3:1), and the base is relatively overperfused (ratio, 0.6:1). Therefore, conditions caused by inhalation of toxic substances primarily affect the apices of the lung.

The lymphatic flow, responsible for clearance of particles from the lung, also plays a key role in the predilection of certain diseases for the upper lobes. Whereas larger inhaled particles in the tracheobronchial airways are removed by the mucociliary system, smaller particles reach the alveoli, from which they are removed by the lymphatic system. Lymphatic particle clearance is relatively decreased in the apices because the lymphatic flow is driven by perfusion as well as respiratory excursion, both of which are relatively deceased in the upper lung zones. This explains why granulomatous disorders, such as tuberculosis or sarcoidosis, appear predominantly in the upper lobes. In addition, metabolic factors, such as regional uptake of oxygen, elimination of carbon dioxide, and pH in the lung, differ due to inequalities of the ventilation-perfusion ratio. These factors contribute to the upper zone predisposition of conditions such as metastatic pulmonary calcification and tuberculosis. Finally, increased mechanical stress of the pulmonary apices caused by a rigid chest cage may result in fibrobullous apical lesions, as in patients with ankylosing spondylitis.

More than one pathway may account for the upper lobe predominance in an individual disease, For example, the distribution of tuberculosis is influenced by the relative overventilation, regional high oxygen tension, and delayed lymphatic clearance in the apices. The attribution of a disease to an underlying physiologic factor is therefore based on the mechanism that is presumably dominant. This article reviews the imaging findings of

TABLE 1: Pulmonary Diseases With Upper Lobe Predominance

Inhaled injurious gases
Smoke inhalation
Centrilobular emphysema
Impaired mucociliary clearance
Cystic fibrosis
Inhaled particulates: pneumoconiosis
Silicosis
Coal worker pneumoconiosis
Berylliosis
Miscellaneous pneumoconioses (hard metal disease, kaolinosis, bauxite pneumoconiosis, fuller's earth disease)
Inhaled antigens
Hypersensitivity pneumonitis
Allergic bronchopulmonary aspergillosis
Chronic eosinophilic pneumonia
Granulomatous diseases
Tuberculosis
Sarcoidosis
Langerhans cell histiocytosis
Bronchocentric granulomatosis
Abnormal perfusion kinetics
Right-sided localized pulmonary edema in acute mitral regurgitation
Neurogenic pulmonary edema
Metabolic diseases
Metastatic pulmonary calcification
Increased mechanical stress
Ankylosing spondylitis

Keywords: lung, pulmonary diseases, upper lobe–predominant disease

DOI:10.2214/AJR.12.8961

Received March 15, 2012; accepted without revision April 5, 2012.

[1]All authors: Department of Radiology, Beth Israel Deaconess Medical Center, Harvard Medical School, 330 Brookline Ave, Boston, MA 02115. Address correspondence to R. L. Eisenberg (rleisenb@bidmc.harvard.edu).

WEB
This is a Web exclusive article.

AJR 2013; 200:W222–W237

0361–803X/13/2003–W222

© American Roentgen Ray Society

the most common pulmonary diseases with upper lobe predominance on the basis of the physiologic background (Table 1).

Inhaled Injurious Gases

Inhaled injurious gases have a relatively higher concentration in the lung apices than in the dependent lung on the basis of the relative apical overventilation. This explains the distribution of findings in the upper lung zones.

Smoke Inhalation

Inhalation of toxic fumes and gases can cause pulmonary damage, depending on the specific toxic agent and the duration of exposure. Typical symptoms of smoke inhalation include cough, shortness of breath, and respiratory failure.

In the acute period up to 48 hours after the toxic exposure, radiographs are frequently normal. There may be evidence of peribronchial wall thickening, as well as subsegmental atelectasis due to narrowed airways from mucosal edema. Subacutely, radiographs may show noncardiogenic edema with diffuse bilateral opacifications that predominantly involve the upper lobes. Overlapping findings of gravity-dependent fluid overload or aspiration pneumonia also may be seen. In most cases, chest radiographs become abnormal 2–5 days after smoke exposure (Fig. 1).

Although CT is rarely used in the acute stage of smoke inhalation, this modality is superb for delineating bronchial wall thickening, diffuse bilateral consolidation, and tree-in-bud pattern that develop within a few hours after exposure (Fig. 1). CT angiography may aid in detecting complications, such as pulmonary embolism. In patients with chronic damage, CT may show bronchiectasis and tracheal stenosis as well as bronchiolitis-related air trapping on expiratory scans.

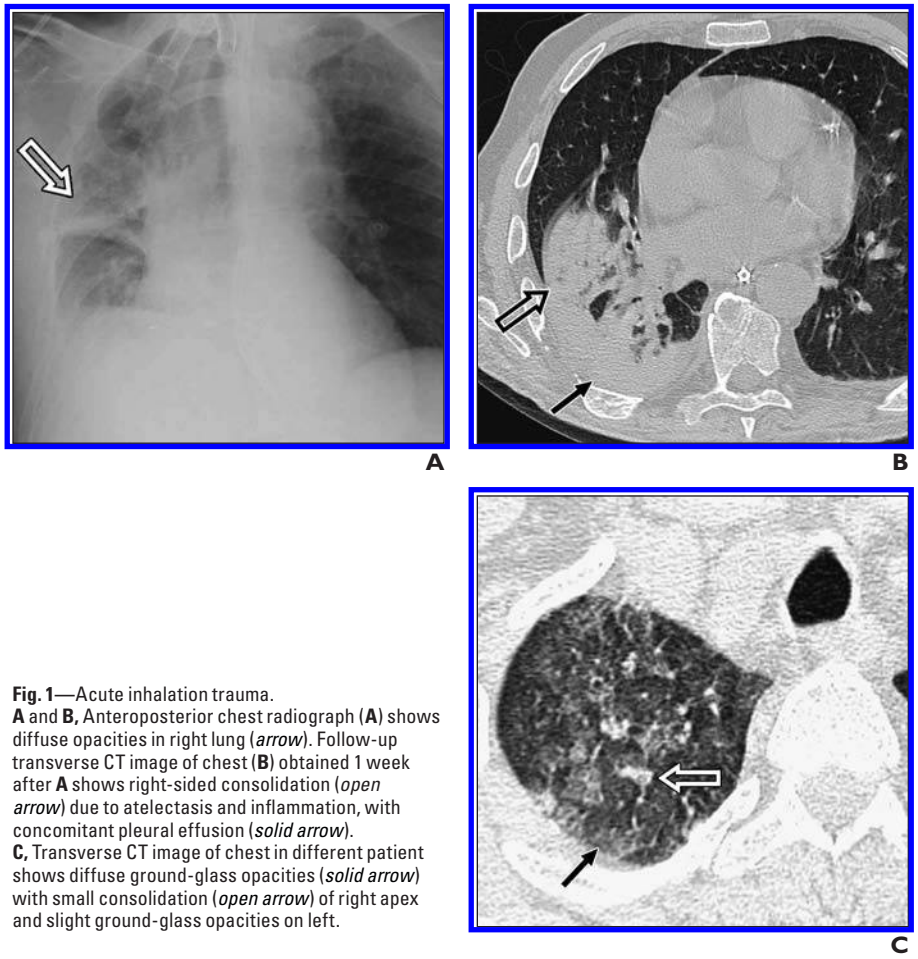

Fig. 1—Acute inhalation trauma.
A and **B,** Anteroposterior chest radiograph (**A**) shows diffuse opacities in right lung (*arrow*). Follow-up transverse CT image of chest (**B**) obtained 1 week after **A** shows right-sided consolidation (*open arrow*) due to atelectasis and inflammation, with concomitant pleural effusion (*solid arrow*).
C, Transverse CT image of chest in different patient shows diffuse ground-glass opacities (*solid arrow*) with small consolidation (*open arrow*) of right apex and slight ground-glass opacities on left.

Downloaded from www.ajronline.org by MIT Libraries on 05/02/24 from IP address 18.116.164.246. Copyright ARRS. For personal use only; all rights reserved

Downloaded from www.ajronline.org by MIT Libraries on 05/02/24 from IP address 18.116.164.246. Copyright ARRS. For personal use only; all rights reserved

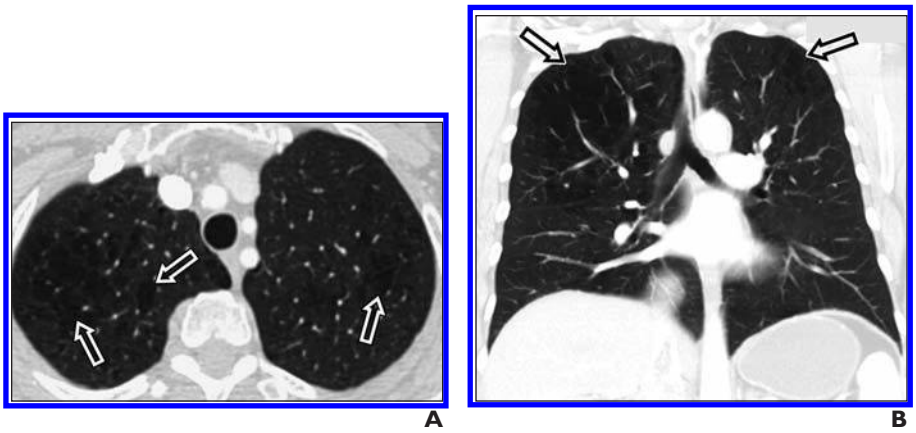

Fig. 2—Centrilobular emphysema.
A and **B,** Transverse (**A**) and coronal (**B**) CT images of chest show multiple areas of low attenuation (*arrows*) surrounded by normal parenchyma and grouped around center of secondary pulmonary lobules in upper lobes.

Centrilobular Emphysema

Emphysema is a permanent abnormal enlargement of airspaces distal to terminal bronchioles that is accompanied by destruction of alveolar walls without fibrosis. Centrilobular emphysema presents with upper lobe predominance and is associated with cigarette smoking. In contrast, panlobular emphysema primarily affects the lower lobes and is associated with α-antitrypsin deficiency.

Emphysema is initially characterized by focal destruction of lung parenchyma, which becomes more diffuse with advancing disease. Radiographic signs include distortion of the vascular structures (focal absence or reduced caliber of pulmonary vessels), focal destruction of lung tissue, and increased lucency of the lung. If emphysema is associated with overinflation, flattening of the hemidiaphragms and an increased retrosternal space may be seen, but these are not pathognomonic findings. Radiography may permit a diagnosis of moderate or severe emphysema, but it is much less sensitive than CT in detecting and evaluating the extent of mild disease. On CT, emphysema is characterized by areas of low attenuation surrounded by normal lung parenchyma (Fig. 2). Mild and moderate centrilobular emphysemas produce multiple small round areas of low attenuation (several millimeters in diameter), usually in the upper lobes (Fig. 2). The lesions have no walls and can be grouped around the center of secondary pulmonary lobules. In contrast, panlobular emphysema produces uniform destruction of the secondary lobule, which results in homogeneous low attenuation that may involve the entire lung. Paraseptal emphysema, another emphysema subtype, may occur as an isolated finding or may be associated with panlobular or centrilobular emphysema. It shows upper lobe predominance and is characterized by multiple bullae in subpleural distribution (Fig. 3).

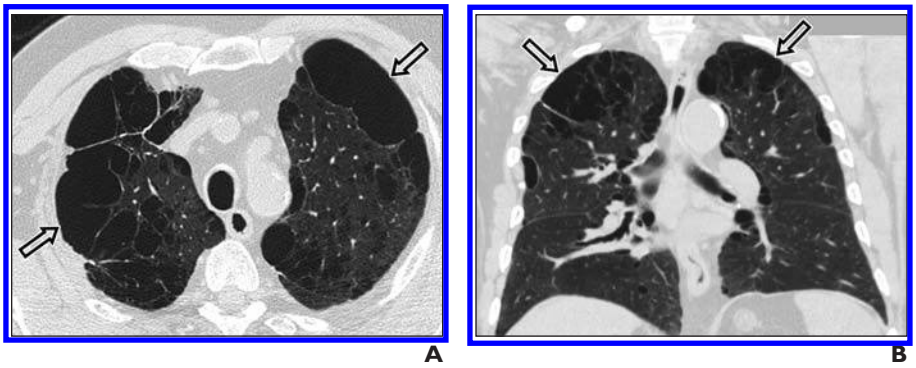

Fig. 3—Paraseptal emphysema.
A and **B,** Transverse (**A**) and coronal (**B**) CT images of chest show destruction of lung parenchyma with distinct bullous changes (*arrows*) that predominate in subpleural regions of upper lobes.

Downloaded from www.ajronline.org by MIT Libraries on 05/02/24 from IP address 18.116.164.246. Copyright ARRS. For personal use only; all rights reserved

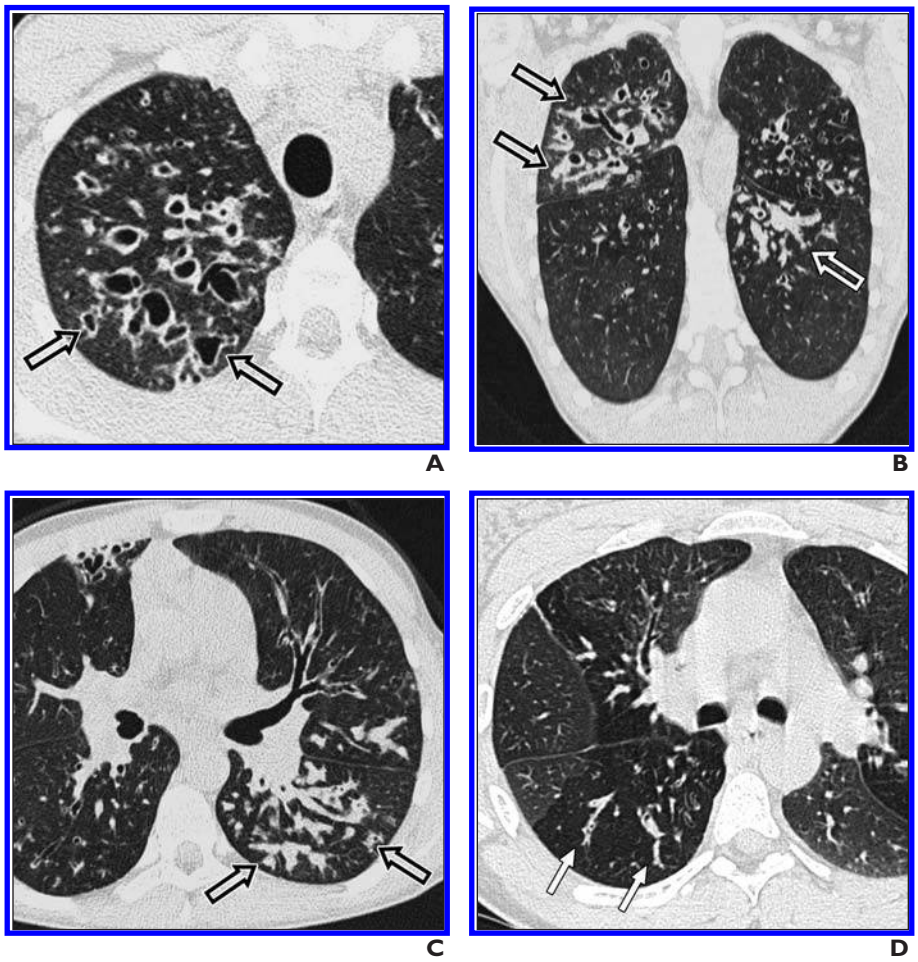

Fig. 4—Cystic fibrosis.
A, Transverse CT image of chest shows distinct bronchial wall thickening and bronchiectasis (*arrows*) surrounded by ground-glass opacities in right lung apex.
B and **C,** Coronal (**B**) and transverse (**C**) CT images of chest show bilateral bronchiectasis and mucous impaction (*arrows*), primarily involving upper lung zones.
D, Transverse CT image of chest obtained in different patient during expiratory maneuver shows distinct mosaic attenuation due to air trapping in small airways disease. There is also typical bronchiectasis with mucous plugging (*arrows*).

On radiographs, advanced cases of multicystic disorders such as lymphangiomyomatosis and Langerhans cell histiocytosis may mimic emphysema. However, CT readily shows the walls of the individual cystic lesions, which differentiate these conditions from emphysema.

Impaired Mucociliary Clearance

Impaired mobilization of secretions predominantly affects the upper lobes, whereas increased respiratory excursion aids in the removal of secretions in the lower lobes. Cystic fibrosis is an autosomal recessive genetic disorder in which a block in the transport of chloride into the bronchial lumen leads to production of abnormally thick mucus. Decreased clearance of this mucus results in mucous plugging in small and large airways and subsequent bacterial infection. Although most patients with cystic fibrosis are diagnosed by the age of 3 years, mild cases may not be evident until adulthood. The clinical diagnosis of cystic fibrosis requires a positive sweat chloride test.

Imaging in patients with cystic fibrosis is primarily important in patient follow-up. Early in the course of disease, radiographs may show hyperinflation of both lungs secondary to obstruction of small airways. As the disease progresses, there is the development of bronchial and peribronchial wall thickening, bronchiectasis, and mucous impaction, usually in the upper lobes. Lobar atelectasis and recurrent pneumonia may be seen in advanced disease. Although radiographs are

Fig. 5—Silicosis. Transverse CT image of chest shows diffusely scattered centrilobular micronodules and multiple subpleural nodules (*arrows*) in upper lobes.

widely used to monitor the pulmonary changes in cystic fibrosis, CT allows reliable confirmation of even slight bronchiectasis with mucous plugging, which has upper lobe predominance (Fig. 4). In addition to bronchial wall and peribronchial thickening, CT shows ground-glass opacities as well as a tree-in-bud pattern of opacities caused by secretions within bronchioles. Expiratory scans may show air trapping (Fig. 4). The differential diagnosis of cystic fibrosis includes Kartagener syndrome (with situs anomalies) and postinfectious bronchiectasis, both of which are usually unilateral and have lower lobe predominance.

Inhaled Particulates: Pneumoconioses

Pneumoconioses are occupational diseases caused by chronic inhalation of particulates. Accumulation of these particulates primarily occurs in the upper lobes where they cannot be removed by the relatively decreased lymphatic flow.

Silicosis

Silicosis is an irreversible lung disease caused by chronic inhalation of crystalline silica (particle size, 0.1–3.0 μm). It occurs most often in people who work in mining, sandblasting, stonecutting, and the manufacture of glass or pottery. The symptoms of silicosis develop about 20 years after initial exposure. Some affected individuals may be asymptomatic, whereas those with severe disease present with cough, dyspnea, and increased sputum. Patients with silicosis also have an increased risk of developing tuberculosis.

At chest radiography, the earliest characteristic findings are small, symmetric nodules (1–3 mm in diameter) that may calcify and predominantly involve the posterior portions of the upper lobes or superior segments of the lower lobes. Hilar and mediastinal lymphadenopathy are common, and peripheral eggshell calcification of enlarged lymph nodes is virtually pathognomonic of silicosis. In complicated disease, the pulmonary nodules increase in size and number and form conglomerate masses (diameter > 1 cm), an appearance known as progressive massive fibrosis. CT is much more sensitive than chest radiography for detecting the diffusely scattered centrilobular micronodules (< 7 mm) (Fig. 5). Chains of subpleural nodules (producing pseudoplaques) and the aggregation of nodules into progressive massive fibrosis also are better delineated on CT (Fig. 5). Masses larger than 4 cm may show central low attenuation due to necrosis. In contrast to the CT appearance in silicosis, aggregation of nodules and subpleural pseudoplaques are much less common in sarcoidosis, tuberculosis, and Langerhans cell histiocytosis. Although asbestosis is a type of pneumoconiosis, it shows lower lobe predominance. This may be explained by the needle shape of asbestos fibers (length, 100 μm; diameter 30 μm), which favors entrapment in the lower lobes. In addition, the lower lobe predisposition may be influenced by indeterminate biochemical factors.

Coal Worker Pneumoconiosis

Coal worker pneumoconiosis is caused by chronic exposure to washed coal (particle size 1–5 μm). Patients may present with cough, dyspnea, and black sputum, and they are more susceptible to tuberculosis. The combination of coal worker pneumoconiosis, pulmonary necrobiotic nodules, and rheumatoid arthritis is known as Caplan syndrome.

Downloaded from www.ajronline.org by MIT Libraries on 05/02/24 from IP address 18.116.164.246. Copyright ARRS. For personal use only; all rights reserved

Downloaded from www.ajronline.org by MIT Libraries on 05/02/24 from IP address 18.116.164.246. Copyright ARRS. For personal use only; all rights reserved

Despite the histopathologic differences, coal worker pneumoconiosis and silicosis share similar imaging findings. Chest radiographs show small symmetric nodules (diameter, 1–5 mm) that may calcify and predominantly involve the upper lobes. Hilar or mediastinal lymphadenopathy is reported in 30% of patients, although eggshell calcifications are much less common than in silicosis. In complicated disease, the pulmonary nodules form conglomerate masses of progressive massive fibrosis. As in silicosis, CT is more sensitive in showing diffusely scattered nodules (diameter, 1–5 mm), which calcify in 30% of patients, or reticulonodular opacities in a perilymphatic distribution. The nodules in coal worker pneumoconiosis tend to be less well defined than in silicosis. As in complicated silicosis, the aggregation of nodules into progressive massive fibrosis is more readily detected on CT than on radiography.

Fig. 6—Berylliosis. Transverse CT image of chest shows diffuse small nodular changes (*arrows*) containing microcalcifications, which primarily involve apical segment of right lower lobe. (Courtesy of Gevenois PA, Université libre de Bruxelles, Brussels, Belgium)

Berylliosis

Berylliosis is a chronic granulomatous lung disease caused by exposure to beryllium dust or fumes among workers in ceramics manufacture, nuclear weapon production, and the aerospace industry. Symptoms usually include dyspnea, cough, fever, anorexia, and weight loss. Proof of granulomatous inflammation at lung biopsy and positive sensitivity testing to beryllium are required to confirm the diagnosis.

Half of patients with chronic disease have normal chest radiographs. Others initially may show diffuse nodular or reticular opacities, and interstitial fibrosis with honeycombing may be apparent in more advanced disease. Symmetric bilateral hilar lymphadenopathy also may be observed. Even on CT, 25% of cases with proven berylliosis appear to be normal. The CT findings of berylliosis are similar to those of sarcoidosis (Fig. 6). Most common are small nodules, predominantly distributed along bronchovascular bundles, and thickened interlobular septa (Fig. 6). Other findings include ground-glass opacities, which may be replaced by microcystic lesions, and fibrosis with honeycombing in the advanced chronic stage. Hilar or mediastinal lymphadenopathy, which always has associated lung disease, is seen in 40% of cases. Both the pulmonary nodules and lymph nodes may contain calcifications. In contrast, hilar lymphadenopathy in sarcoidosis may occur without lung disease, and ground-glass opacities are less common.

Miscellaneous Pneumoconioses

Hard metal lung disease is a rare form of pneumoconiosis that is primarily caused by exposure to cobalt dust. Most patients present with chronic cough or dyspnea. Chest radiographs show nonspecific findings, such as linear and nodular opacities, which are occasionally accompanied by lymphadenopathy. In advanced stage disease, there is pulmonary fibrosis that has upper lobe predominance. On CT, bronchiolitis obliterans is the earliest manifestation of disease. There also may be bilateral ground-glass opacities or consolidations, reticular opacities, and traction bronchiectasis, all of which have upper lobe predominance. In advanced disease, parenchymal distortion and honeycombing may be seen. Hard metal lung disease may resemble usual interstitial pneumonia or nonspecific interstitial pneumonitis. Therefore, the diagnosis should be based on a combination of occupational, clinical, and radiologic findings and then confirmed by the pathognomonic histopathologic appearance of giant cell interstitial pneumonia.

Among the rare pneumoconioses are kaolinosis from inhalation of dust containing kaolin, the main component in porcelain; bauxite pneumoconiosis (Shaver disease), caused by exposure to bauxite fumes containing aluminum and silica particulates; and fuller's earth disease, from prolonged exposure to calcium montmorillonite (fuller's earth) used in absorbents and filters.

Downloaded from www.ajronline.org by MIT Libraries on 05/02/24 from IP address 18.116.164.246. Copyright ARRS. For personal use only; all rights reserved

Fig. 7—Acute hypersensitivity reaction to calcium sulfate in gypsum exposure. Transverse CT image of chest shows diffuse bilateral upper lobe airspace nodules, reflecting alveolitis without signs of lung fibrosis.

Inhaled Antigens

Predilection for the upper lobes in antigen inhalation results from relative apical overventilation. Because inhalation of antigens is associated with an exaggerated immune response (hypersensitivity), potential granulomatous reaction primarily affects the upper lobes due to delayed lymphatic clearance in these areas.

Hypersensitivity Pneumonitis

Hypersensitivity pneumonitis, also known as extrinsic allergic alveolitis, refers to a group of allergic lung diseases caused by chronic inhalation of various organic and chemical antigens. The most common forms are farmer lung and bird fancier lung. The acute symptoms of hypersensitivity pneumonitis develop 4–12 hours after dust exposure and include cough, fever, and myalgia. In chronic disease, patients may have cough, progressive dyspnea, fatigue, and weight loss.

In the acute phase, chest radiographs are normal in 90% of cases. In subacute disease, radiographs may show poorly defined small nodules or lung opacifications. In the chronic stage, radiographs show lung fibrosis with architectural distortion.

CT is more sensitive than radiography in detecting hypersensitivity pneumonitis and following its evolution. It appears acutely as small (< 5 mm diameter) ill-defined centrilobular nodules and bilateral airspace consolidations that have a mid and upper zone distribution (Fig. 7). In the subacute stage, there are patchy ground-glass opacities with ill-defined centrilobular nodules, which can progress to heterogeneous ground-glass attenuation (Fig. 8). Mosaic attenuation is also a common finding, and air trapping may be seen on expiratory scans. In chronic hypersensitivity pneumonitis, lung fibrosis produces honeycombing, traction bronchiectasis, and architectural distortion. The characteristic appearance of hypersensitivity pneumonitis is different from idiopathic pulmonary fibrosis, which shows subpleural and basal reticular changes, and from nonspecific interstitial pneumonia, in which there is only minimal or

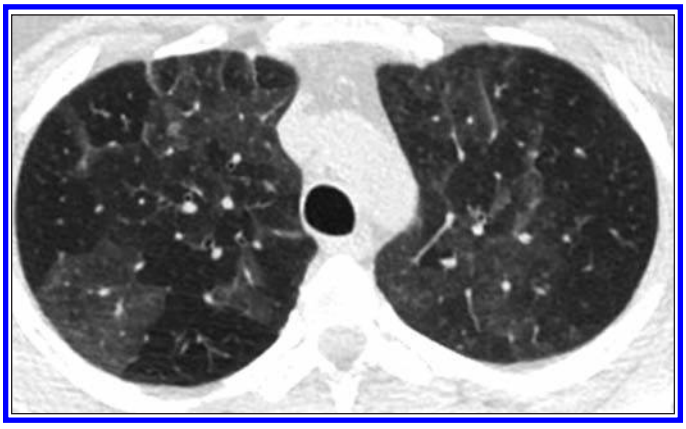

Fig. 8—Hypersensitivity pneumonitis (subacute stage). Transverse CT image of chest shows diffuse bilateral ground-glass opacities that cause geographic pattern of mosaic attenuation without architectural distortion, predominantly involving upper lobes.

absent honeycombing. Respiratory bronchiolitis–interstitial lung disease may have similar imaging features, but this condition has a strong association with cigarette smoking.

Allergic Bronchopulmonary Aspergillosis

Allergic bronchopulmonary aspergillosis is a hypersensitivity reaction that is usually caused by *Aspergillus fumigatus* and is typically seen in patients with asthma or cystic fibrosis. Clinical diagnostic criteria include peripheral blood eosinophilia, positive skin testing for *Aspergillus* antigen, and increased serum IgE levels. Clinical symptoms include wheezing, expectoration of brown mucous plugs, chest pain, and fever.

Radiographic findings in allergic bronchopulmonary aspergillosis include tubular mucoid impaction (finger-in-glove sign produced by increased opacity in a bronchial distribution), central bronchiectasis, and consolidations (Fig. 9). CT findings initially include transient opacities and tree-in-bud pattern (centrilobular nodules and branching linear structures). In advanced disease, CT provides delineation of cystic, saccular, or varicoid bronchiectasis and mucoid impaction due to hyphal masses within bronchi and bronchioles (gloved finger sign) (Fig. 9). Mucoid impaction may cause bronchial obstruction and postobstructive atelectasis. In about 30% of patients, the impacted mucus is highly opaque or appears calcified on CT

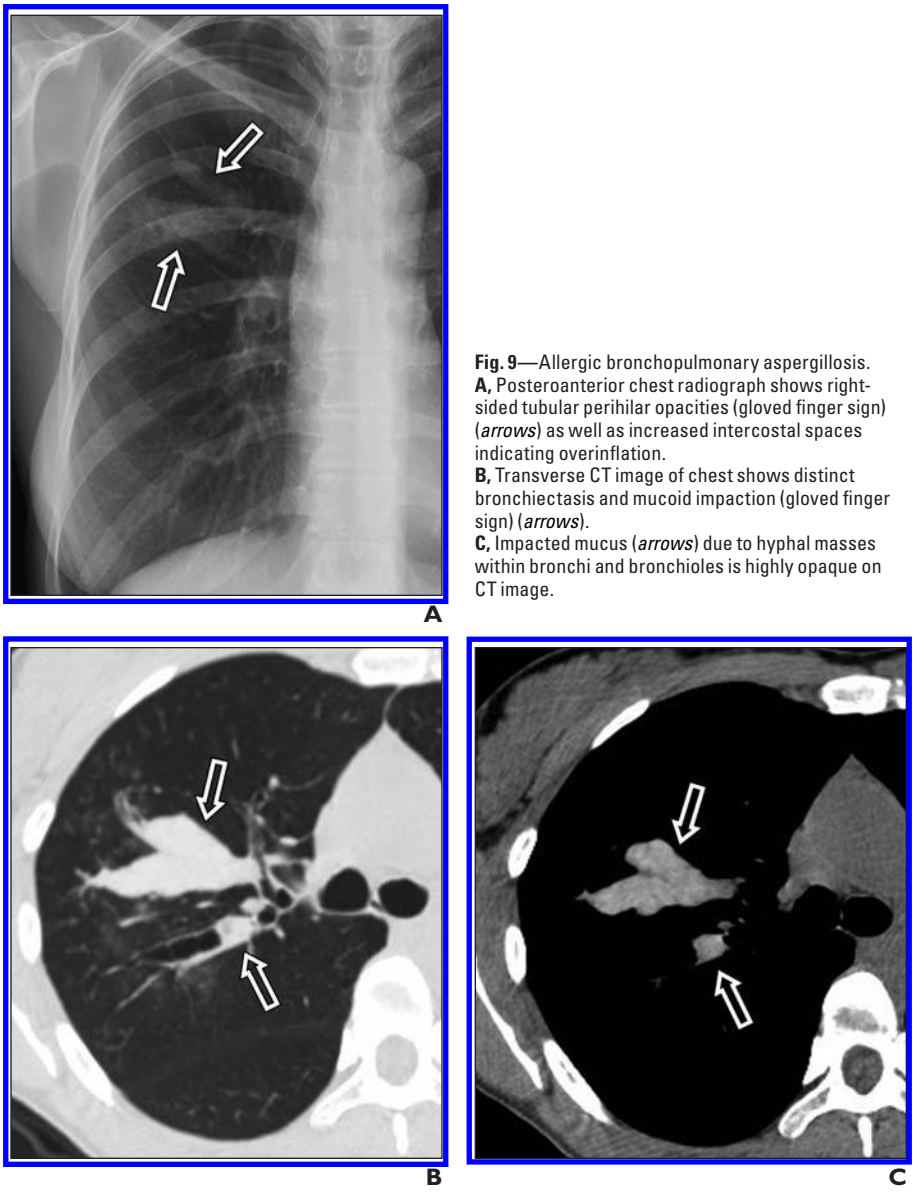

Fig. 9—Allergic bronchopulmonary aspergillosis.
A, Posteroanterior chest radiograph shows right-sided tubular perihilar opacities (gloved finger sign) (*arrows*) as well as increased intercostal spaces indicating overinflation.
B, Transverse CT image of chest shows distinct bronchiectasis and mucoid impaction (gloved finger sign) (*arrows*).
C, Impacted mucus (*arrows*) due to hyphal masses within bronchi and bronchioles is highly opaque on CT image.

Downloaded from www.ajronline.org by MIT Libraries on 05/02/24 from IP address 18.116.164.246. Copyright ARRS. For personal use only; all rights reserved

(Fig. 9). CT is valuable for differentiating conditions that may be associated with bronchial obstruction and mucoid impaction, such as carcinoid tumor, broncholithiasis, and bronchial atresia. In patients with cystic fibrosis, clinical criteria are important to confirm the presence of superimposed allergic bronchopulmonary aspergillosis.

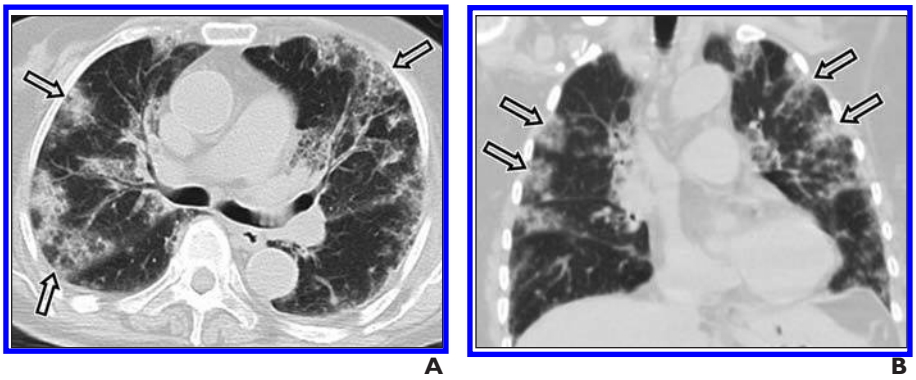

Fig. 10—Chronic eosinophilic pneumonia.
A and **B,** Transverse (**A**) and coronal (**B**) CT images of chest show consolidations (*arrows*) that predominately show peripheral bandlike appearance in upper lobes.

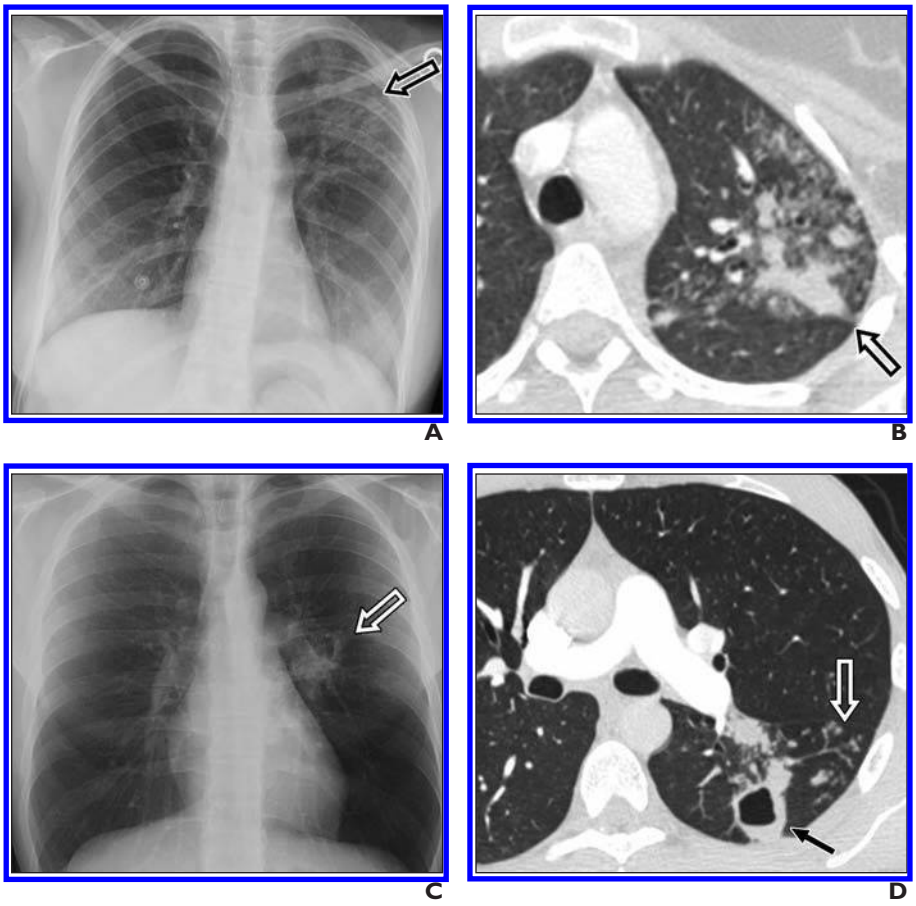

Fig. 11—Recurrent tuberculosis.
A and **B,** Posteroanterior chest radiograph (**A**) and transverse CT image (**B**) of chest show patchy heterogeneous consolidation in left upper lobe (*arrows*).
C and **D,** Posteroanterior chest radiograph (**C**) shows opacity in perihilar region (*arrow*); transverse CT image of chest (**D**) confirms changes as cavitation (*solid arrow*) and also shows surrounding tree-in-bud pattern (*open arrow*).

Downloaded from www.ajronline.org by MIT Libraries on 05/02/24 from IP address 18.116.164.246. Copyright ARRS. For personal use only; all rights reserved

Downloaded from www.ajronline.org by MIT Libraries on 05/02/24 from IP address 18.116.164.246. Copyright ARRS. For personal use only; all rights reserved

Chronic Eosinophilic Pneumonia

Chronic eosinophilic pneumonia is an idiopathic condition that most commonly affects middle-aged patients, about half of whom have asthma. Clinically, it is characterized by dyspnea, cough, malaise, and fever. There is usually moderate peripheral blood eosinophilia and a high percentage of eosinophils in the bronchoalveolar lavage.

Radiographs in chronic eosinophilic pneumonia show bilateral peripheral consolidations with upper zone predominance. This is distinct from acute eosinophilic pneumonia, which mimics pulmonary edema and predominantly affects the lower lobes. CT in chronic eosinophilic pneumonia shows nonsegmental peripheral airspace consolidation resembling bandlike opacities parallel to the pleural surface (photographic negative shadow of pulmonary edema), primarily in the upper lobes (Fig. 10). This characteristic distribution is most frequently detected on CT, which also is valuable for monitoring the response to corticosteroid therapy. Cryptogenic organizing pneumonia also may show peripheral consolidations, but it is more commonly found in the lower lobes. In Loeffler syndrome, the peripheral opacities are much more transient.

Granulomatous Diseases

The upper lobe predominance of granulomatous diseases is strongly determined by delayed lymphatic clearance in the apices. Depending on the specific condition, there also may be a contribution from the inhalation pathway with relative apical overventilation.

Tuberculosis

Tuberculosis is an airborne infectious granulomatous disease caused by *Mycobacterium tuberculosis*. Patients with active pulmonary tuberculosis may be asymptomatic or have dry cough, fever, fatigue, weight loss, night sweats, or bloody sputum. Primary tuberculosis most commonly occurs in children and presents with unilateral hilar and/or mediastinal lymphadenopathy in 90–95% of patients and airspace consolidation (without upper lung predominance) in about 70% of patients. Recurrent tuberculosis (reinfection and postprimary tuberculosis due to reactivation) predominantly involves the apical and posterior segments of the upper lobes and the superior segments of the lower lobes because of the relatively higher oxygen tension and delayed lymphatic drainage in these areas.

Radiographically, recurrent tuberculosis appears as a focal or patchy heterogeneous consolidation and may produce poorly defined nodular opacities that cavitate (Fig. 11). Cavitation, the radiographic hallmark of recurrent tuberculosis, is evident in 20–45% of patients (Fig. 11). Upper lobe fibrosis also occurs.

CT shows centrilobular small nodules and branching linear and nodular opacities (tree-in-bud sign), which reflect the endobronchial spread of infection in recurrent tuberculosis (Fig. 11). CT may also show patchy or lobular areas of consolidation, interlobular thickening, and cavitation of nodules that may heal as a fibrotic lesion (Fig. 11). Hilar or mediastinal lymphadenopathy is seen in only 5–10% of patients with recurrent tuberculosis, and pleural effusion occurs in 15–20%. CT is of value in showing such complications of tuberculosis as empyema, bronchopleural fistula, and pulmonary fibrosis as well as postinfectious tuberculosis findings (Fig. 12). The CT differential diagnosis of recurrent tuberculosis includes sarcoidosis and silicosis. Compared with end-stage sarcoidosis, recurrent tuberculosis is usually not associated with lymphadenopathy. Tuberculosis must be excluded by culture in patients with silicosis because there is an increased incidence of tuberculosis in progressive massive fibrosis.

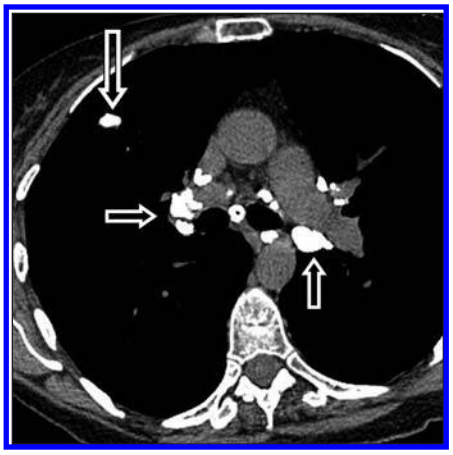

Fig. 12—Postinfectious inactive tuberculosis. Transverse CT image of chest shows multiple calcified mediastinal and hilar lymph nodes (*short arrows*) as well as calcified parenchymal opacity (*long arrow*).

As an interesting side note, the host's position affects the distribution of tuberculosis as

Downloaded from www.ajronline.org by MIT Libraries on 05/02/24 from IP address 18.116.164.246. Copyright ARRS. For personal use only; all rights reserved

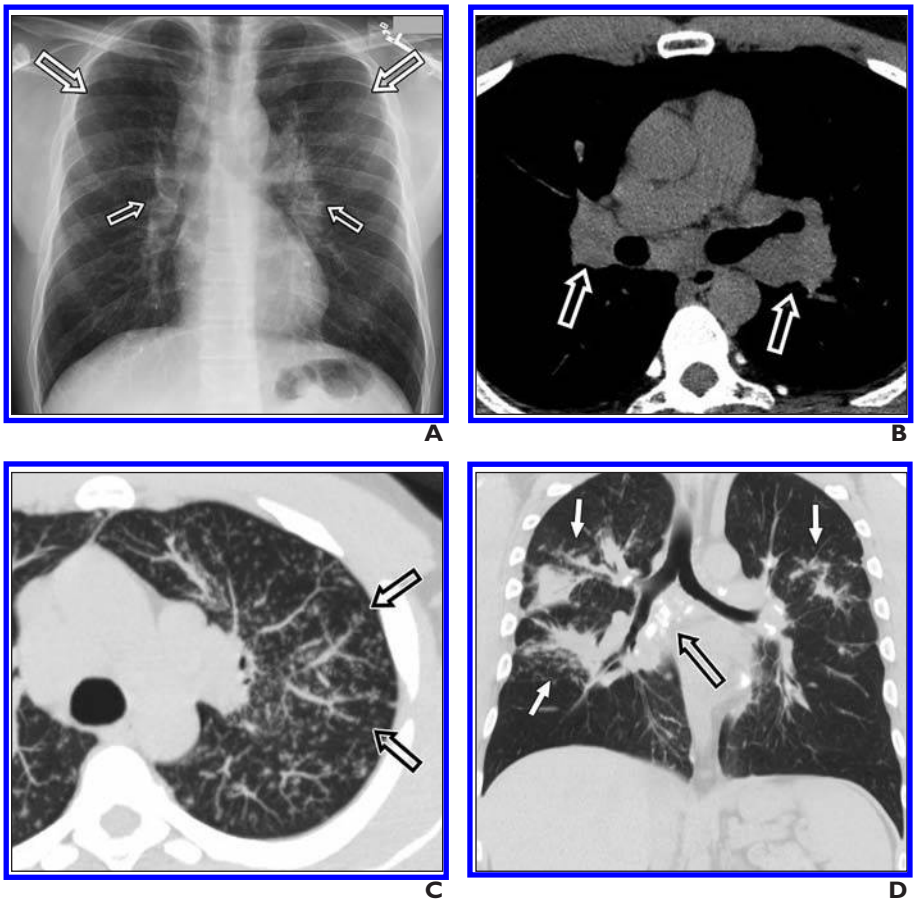

Fig. 13—Pulmonary sarcoidosis.
A, Posteroanterior chest radiograph shows hilar enlargement (*small arrows*) and diffuse reticulonodular opacities (*large arrows*), predominantly in upper lung zones.
B, Transverse CT image of chest shows bilateral hilar lymphadenopathy (*arrows*), virtually without calcification.
C, Transverse CT image of chest also shows innumerable micronodules in peribronchovascular distribution (*arrows*).
D, Coronal CT image of chest in different patient shows multiple calcified mediastinal and hilar lymph nodes (*open arrow*) as well as pulmonary opacities that have masslike appearance (*solid arrows*).

observed in animals. In bats hanging headfirst from tree branches or hollows, tuberculosis in the lung is observed in the lower lung zones, in contrast to upper lobe predominance in upright ambulating humans.

Sarcoidosis

Sarcoidosis is a multisystem inflammatory disease that is characterized by noncaseating granulomas. Although its cause remains unknown, studies have suggested an association of sarcoidosis with genetic and immunologic mechanisms as well as infectious antigens and environmental exposures. The lung is most commonly involved, but sarcoidosis may affect the joints, eyes, kidneys, and skin. Most patients are 25–40 years old. Many patients with sarcoidosis are asymptomatic, with the disease an incidental finding on chest radiography. Others have persistent cough, dyspnea, malaise, fever, or night sweats. The most common complication of sarcoidosis is respiratory failure due to pulmonary fibrosis.

The characteristic radiographic finding in sarcoidosis is bilateral enlargement of hilar and mediastinal lymph nodes, which is seen in up to 90% of patients (Fig. 13). About 20% of patients have diffuse reticulonodular opacities, which predominantly involve the upper lung zones (Fig. 13). The nodal enlargement typically resolves as the parenchymal disease develops, unlike in lymphoma or tuberculosis.

On CT, hilar and mediastinal lymphadenopathy may show amorphous, punctuate, or eggshell calcification (Fig. 13). On CT studies, interstitial lung disease typically manifests as

Downloaded from www.ajronline.org by MIT Libraries on 05/02/24 from IP address 18.116.164.246. Copyright ARRS. For personal use only; all rights reserved

small nodules (1–5 mm) with a peribronchovascular distribution extending from the hilum to the periphery along with interlobular septal thickening (Fig. 13). The micronodular changes may appear in a cluster pattern. Small airway involvement, including nodular bronchial and bronchiolar wall thickening, may cause a pattern of mosaic attenuation on CT. Other CT manifestations of sarcoidosis include ground-glass opacities and an alveolar pattern of airspace nodules and consolidation with air bronchograms (Fig. 13). In complicated disease, the sarcoid nodules may coalesce to form masslike lesions causing progressive massive fibrosis, and architectural distortion and honeycombing may be seen (Fig. 14). Cysts and cavitations caused by necrotizing sarcoidal angiitis may be found. The findings in sarcoidosis may be mimicked by silicosis or berylliosis, although patients with these two conditions have a distinctive occupational history. In Langerhans cell histiocytosis, there is only minimal lymphadenopathy.

Langerhans Cell Histiocytosis

Langerhans cell histiocytosis is a granulomatous disorder that occurs almost exclusively in smokers and has no sex predominance. Because of the inhalational component, the relatively overventilated upper lung zones are predominantly involved. Most patients are 20–40 years old and present with cough, dyspnea, and fatigue.

The radiographic findings of pulmonary Langerhans cell histiocytosis include diffuse symmetric nodular opacities and cysts, with upper lobe predominance (Fig 15). CT is more sensitive than radiography in showing of the typical ill-defined nodules (1–10 mm) and cysts (1–3 cm) surrounded by normal lung parenchyma in a heavy smoker (Fig. 15). There may be few or innumerable nodules, usually with irregular margins and in a centrilobular or peribronchial distribution. Some nodules progress to thick-walled cavities. The cysts in Langerhans cell histiocytosis may have thin or thick walls; have a spherical, lobulated, septate, or bizarre shape; and exist alone or with associated nodules (Fig. 15). In 25% of patients, pneumothorax occurs as a complication of cyst rupture during the course of disease. Unlike Langerhans cell histiocytosis, in lymphangiomyomatosis, spherical cysts are found diffusely throughout the lungs and the condition affects women almost exclusively.

Bronchocentric Granulomatosis

Bronchocentric granulomatosis is a rare necrotizing granulomatous inflammation of the bronchial and bronchiolar epithelium. About one third of affected patients have asthma and eosinophilia. This condition also can occur with allergic bronchopulmonary aspergillosis or as a response to infection with mycobacteria, fungi, or *Echinococcus* species. Patients may have fever, night sweats, cough, and dyspnea.

Radiographic findings are usually unilateral (75% of cases) and predominantly involve the upper lung zones (60%) but are nonspecific. They can be conveniently separated into two patterns: multiple or solitary masses (60% of cases) associated with mucoid impaction, which

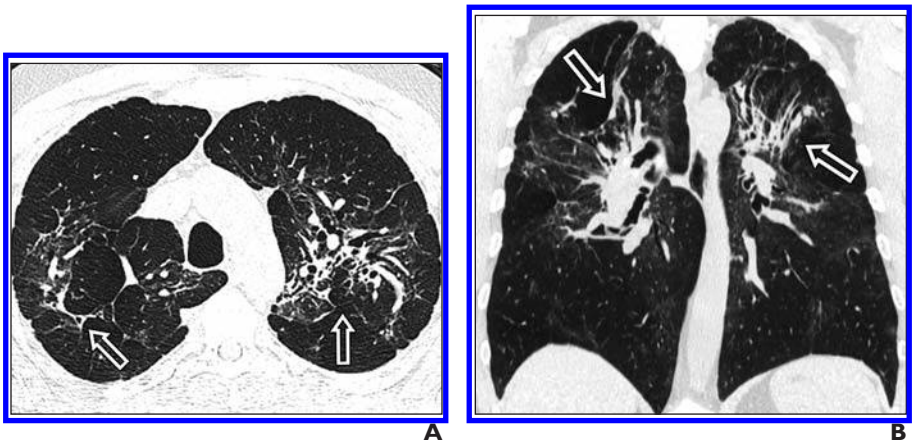

Fig. 14—Distortion of pulmonary architecture in sarcoidosis.
A and **B**, Transverse (**A**) and coronal (**B**) CT images of chest show bilateral ground-glass opacities and parenchymal distortion (*arrows*) with moderate traction bronchiectasis, all predominantly involving upper lobes.

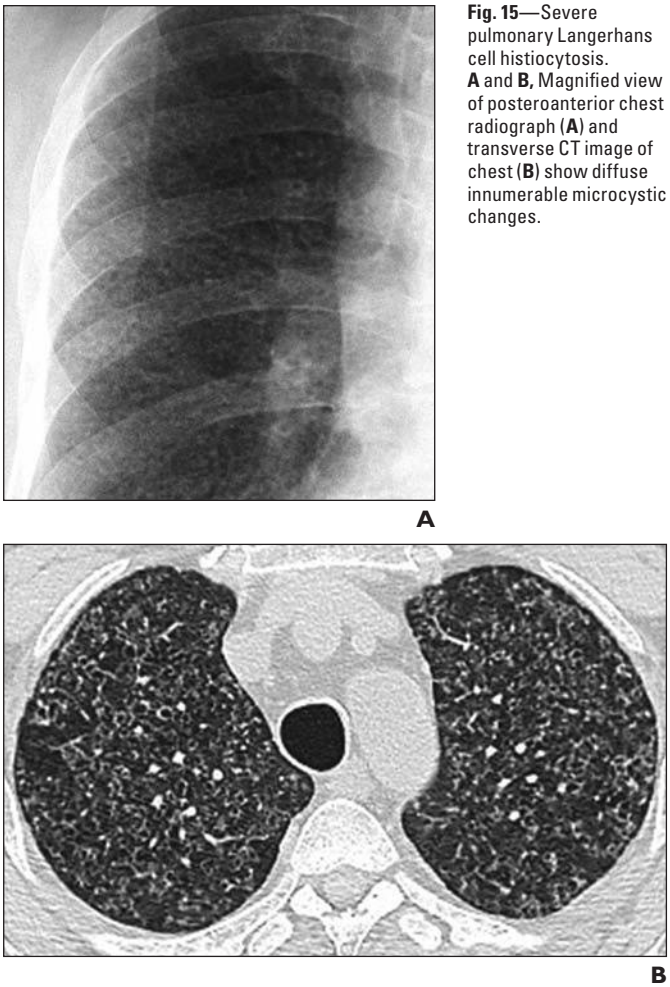

Fig. 15—Severe pulmonary Langerhans cell histiocytosis. **A** and **B,** Magnified view of posteroanterior chest radiograph (**A**) and transverse CT image of chest (**B**) show diffuse innumerable microcystic changes.

manifests as branching opacities or atelectasis; and ill-defined parenchymal consolidations (25%). The CT appearance of bronchocentric granulomatosis includes thick-walled ectatic bronchi and bronchioles, eventually with mucoid impaction, focal masses that may show cavitation, and lobar consolidations (Fig. 16). Hilar lymphadenopathy and pleural disease are infrequently seen. Because of the nonspecific imaging findings, histologic confirmation is required for diagnosis and to differentiate bronchocentric granulomatosis from metastatic disease, septic abscesses, and lymphoma. CT is particularly important for monitoring the response to corticosteroid therapy in this condition.

Abnormal Perfusion Kinetics

Abnormal arterial perfusion kinetics based on cardiovascular disease may account for disorders that primarily affect the right upper lobe.

Right-Sided Localized Edema

Pulmonary edema localized to the right upper lobe has been described rarely in patients with acute mitral regurgitation. It is most likely the result of an asymmetric increase in the hydrostatic pressure of the right upper lung caused by asymmetric blood flow from the left atrium. A regurgitant jet targeted at the orifice of the right upper pulmonary vein produces the increased IV pressure that promotes the development of edema.

Chest radiographs are usually sufficient for detection and monitoring of localized edema, which appears as perihilar homogeneous airspace consolidations in the right upper lobe. The heart is usually enlarged, and there may be signs of left atrial enlargement on posteroanterior radiographs, such as bulging of the left atrial appendage and splaying of the subcarinal angle

Downloaded from www.ajronline.org by MIT Libraries on 05/02/24 from IP address 18.116.164.246. Copyright ARRS. For personal use only; all rights reserved

Downloaded from www.ajronline.org by MIT Libraries on 05/02/24 from IP address 18.116.164.246. Copyright ARRS. For personal use only; all rights reserved

Fig. 16—Bronchocentric granulomatosis. Transverse CT image of chest shows unilateral solitary mass (*arrow*) in right lung with nonspecific appearance.

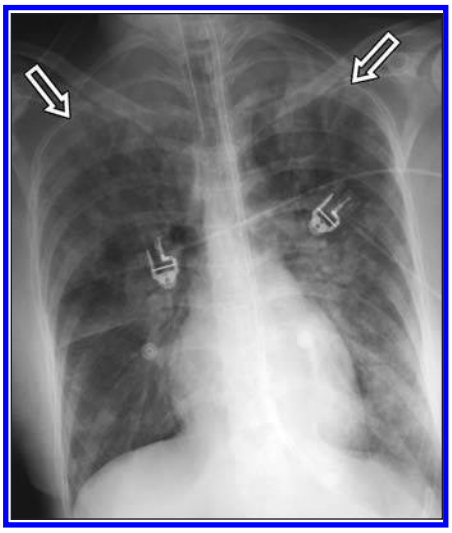

Fig. 17—Neurogenic pulmonary edema in intracranial hemorrhage. Anteroposterior chest radiograph shows bilateral airspace consolidations (*arrows*), which predominate in upper lung zones. There is enlargement of central pulmonary artery, although heart size is normal.

(> 75°). At times, there may be an incorrect initial diagnosis of pneumonia because the possibility of cardiac disease associated with unilateral pulmonary findings is not considered.

Neurogenic Pulmonary Edema

Neurogenic pulmonary edema is seen in up to 50% of patients with severe brain insult related to trauma, hemorrhage, stroke, or epilepsy. The exact pathways of neurogenic pulmonary edema are not well understood. It probably involves a combination of increased hydrostatic pressure edema and permeability edema on the basis of intense activation of the sympathetic nervous system. The upper zone predominance may be explained by abrupt alterations in normal pulmonary perfusion.

Chest radiography shows bilateral rather homogeneous airspace consolidations, which predominate at the apices in about 50% of cases (Fig. 17). The heart is usually normal in size, and pleural effusions are commonly absent. Chest radiography may be sufficient for detection and monitoring because the radiologic findings in neurogenic pulmonary edema usually disappear within 1–2 days. CT may be used to identify additional trauma-associated findings, such as pulmonary contusion.

Metabolic Diseases

Predilection for calcification in the upper lobes results from the relative alkaline environment in these areas on the basis of relative apical overventilation and hence lower partial pressures of CO_2. Metastatic pulmonary calcification is a consequence of calcium deposition in normal pulmonary parenchyma. It may occur in patients with hyperparathyroidism, chronic renal failure, IV calcium therapy, and osteolysis due to metastases or multiple myeloma. Metastatic pulmonary calcification is usually asymptomatic, although respiratory failure infrequently occurs.

Although commonly reported on autopsy in patients with chronic renal failure, metastatic pulmonary calcification is rarely diagnosed on chest radiographs. There may be diffuse or focal ill-defined nodular and linear opacities, which are often mistaken for pneumonia or edema (Fig. 18). CT shows centrilobular fluffy ground-glass nodular opacities, which contain foci of calcification (3–10 mm) in a punctuate, ringlike, or cotton ball pattern and have upper lung predominance. Severe interstitial calcification can result in dense consolidation, which eventually results in fibrosis. At times, there may be calcified vessels in the chest wall. Metastatic pulmonary calcification differs from alveolar microlithiasis, in which the diffuse calcifications are small (1 mm) and have lower lobe predominance. In contrast to silicosis, metastatic calcification is usually not associated with mediastinal lymphadenopathy and subpleural lesions.

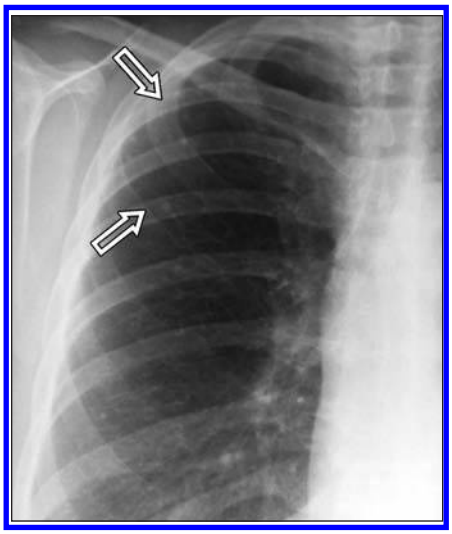

Fig. 18—Metastatic pulmonary calcification. Posteroanterior chest radiograph shows multiple punctuate calcifications (*arrows*) in upper lung zones. Patient had no history of tuberculosis or varicella pneumonia.

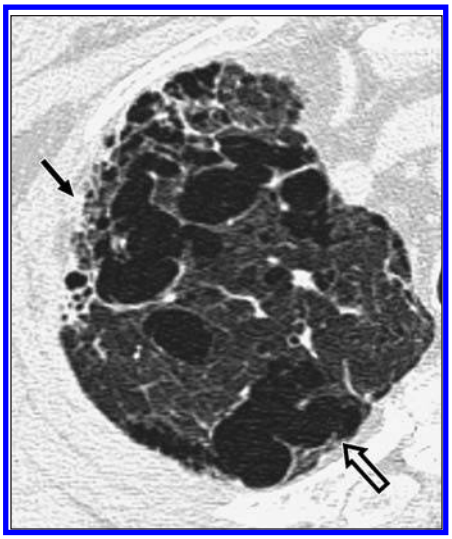

Fig. 19—Ankylosing spondylitis. Transverse CT image of chest shows apical fibrobullous disease that includes subpleural fibrosis (*solid arrow*) as well as bullous changes (*open arrow*).

Increased Mechanical Stress

Physiologically, mechanical stresses are greatest at the apices due to a relatively immobile chest wall and larger alveoli in these areas that result from distortion of the lung by its own weight. Increased mechanical stress is found in patients with abnormally restricted chest wall mobility and may result in apical pulmonary disease.

Ankylosing spondylitis is an idiopathic inflammatory arthritis that has a genetic contribution (96% of patients are *HLA-B27*-positive). This condition is characterized by spinal ankylosis with syndesmophyte formation and bilateral sacroiliac joint disease. Ankylosing spondylitis has a male predominance and manifests in early adulthood, typically with insidious back pain. Restrictive ventilatory impairment may develop because of thoracic spine ankylosis, whereas pleuropulmonary findings develop in only 1–2% of patients. An important diagnostic observation is that ankylosis always precedes lung disease.

On chest radiographs, there are symmetric apical fibrobullous lesions and bronchiectasis. Cavities that develop within the fibrotic lung may be colonized by *A. fumigatus*. CT may reveal alterations at the lung apices that are undetected on radiography. These include apical fibrobullous disease, bronchial wall thickening and bronchiectasis, and cavities (Fig. 19). In addition, CT may show dilatation of the ascending aorta that is frequently present in such patients. Other conditions that may produce a similar pulmonary appearance, such as tuberculosis, sarcoidosis, and silicosis, do not cause spinal ankylosis. Moreover, sarcoidosis is characterized by bronchovascular thickening along with small nodules, and patients with silicosis typically have a relevant occupational history.

Selected Reading

1. Chong S, Lee KS, Chung MJ, et al. Pneumoconiosis: comparison of imaging and pathologic findings. *RadioGraphics* 2006; 26:59–77
2. Criado E, Sánchez M, Ramírez J, et al. Pulmonary sarcoidosis: typical and atypical manifestations at high-resolution CT with pathologic correlation. *RadioGraphics* 2010; 30:1567–1586
3. Eisenberg RL. Chest patterns. In: Eisenberg RL. *Clinical imaging: an atlas of differential diagnosis*. Philadelphia, PA: Lippincott Williams & Wilkins, 2010
4. Gluecker T, Capasso P, Schnyder P, et al. Clinical and radiologic features of pulmonary edema. *RadioGraphics* 1999; 19:1507–1531
5. Gurney JW, Schroeder BA. Upper lobe lung disease: physiologic correlates. *Radiology* 1988; 167:359–366
6. Hirschmann JV, Pipavath SN, Godwin JD. Hypersen-

Downloaded from www.ajronline.org by MIT Libraries on 05/02/24 from IP address 18.116.164.246. Copyright ARRS. For personal use only; all rights reserved

sitivity pneumonitis: a historical, clinical, and radiologic review. *RadioGraphics* 2009; 29:1921–1938
7. Jeong YJ, Kim KI, Seo IJ, et al. Eosinophilic lung diseases: a clinical, radiologic, and pathologic overview. *RadioGraphics* 2007; 27:617–637
8. Jeong YJ, Lee KS. Pulmonary tuberculosis: up-to-date imaging and management. *AJR* 2008; 191:834–844
9. Kim KI, Kim CW, Lee MK, et al. Imaging of occupational lung disease. *RadioGraphics* 2001; 21:1371–1391
10. Litmanovich D, Boiselle PM, Bankier AA. CT of pulmonary emphysema: current status, challenges, and future directions. *Eur Radiol* 2009; 19:537–551
11. Martinez S, Heyneman LE, McAdams HP, et al. Mucoid impactions: finger-in-glove sign and other CT and radiographic features. *RadioGraphics* 2008; 28:1369–1382
12. Schnyder PA, Sarraj AM, Duvoisin BE, et al. Pulmonary edema associated with mitral regurgitation: prevalence of predominant involvement of the right upper lobe. *AJR* 1993; 161:33–36

Downloaded from www.ajronline.org by MIT Libraries on 05/02/24 from IP address 18.116.164.246. Copyright ARRS. For personal use only; all rights reserved

This article has been cited by:

1. Ryan B. Ko, Jonathan A. Abelson, Dominik Fleischmann, John D. Louie, Gloria L. Hwang, Daniel Y. Sze, Emil Schüler, Kayla N. Kielar, Peter G. Maxim, Quynh-Thu Le, Wendy H. Hara, Maximilian Diehn, Nishita Kothary, Billy W. Loo. 2024. Pulmonary interstitial lymphography: A prospective trial with potential impact on stereotactic ablative radiotherapy planning for early-stage lung cancer. *Radiotherapy and Oncology* **191**, 110079. [Crossref]
2. Bruce J. Kimura, Pamela M. Resnikoff, Eric M. Tran, Pranay R. Bonagiri, Samantha R. Spierling Bagsic. 2022. Simplified Lung Ultrasound Examination and Telehealth Feasibility in Early SARS-CoV-2 Infection. *Journal of the American Society of Echocardiography* **35**:10, 1047-1054. [Crossref]
3. Michael P. Mohning, John Caleb Richards, Tristan J. Huie. 2019. Idiopathic pulmonary fibrosis: the radiologist's role in making the diagnosis. *The British Journal of Radiology* **92**:1099. . [Crossref]
4. Binit Sureka, Mahesh Kumar Mittal, Brij Bhushan Thukral. 2013. Differential Diagnosis of Upper Lobe–Predominant Diseases of the Lung. *American Journal of Roentgenology* **201**:3, W518-W518. [Citation] [Full Text] [PDF] [PDF Plus]

Downloaded from www.ajronline.org by MIT Libraries on 05/02/24 from IP address 18.116.164.246. Copyright ARRS. For personal use only; all rights reserved